Lewis Acid-Assisted Isotopic ^{18}F-^{19}F Exchange in BODIPY Dyes: Facile Generation of Positron Emission Tomography/Fluorescence Dual Modality Agents for Tumor Imaging

Shuanglong Liu[1], Tzu-Pin Lin[2], Dan Li[1,3], Lauren Leamer[2], Hong Shan[3], Zibo Li[*,1], François P. Gabbaï[*,2], Peter S. Conti[1]

1. Molecular Imaging Center, Department of Radiology, University of Southern California, Los Angeles 90033, USA.
2. Department of Chemistry, Texas A&M University, College Station, Texas 77843, USA.
3. Department of Radiology, The Third Affiliated Hospital of Sun Yat-sen University, Guangzhou 510630, China.

SUPPLEMENTARY INFORMATION

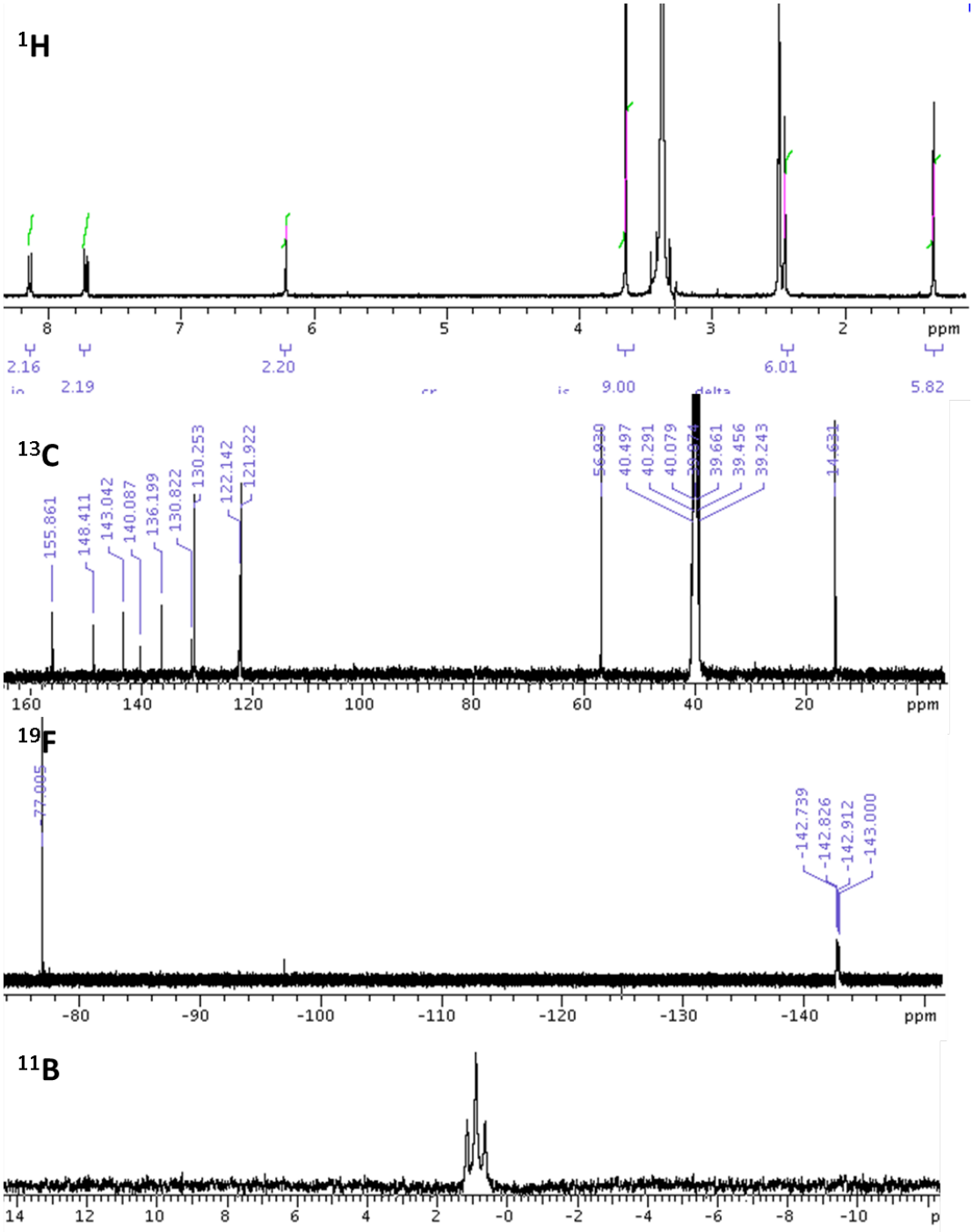

Figure S1. ^{1}H, ^{13}C, ^{19}F, and ^{11}B NMR spectra of [**1**][OTf].

UV-vis and fluorescence measurements of [1][OTf].UV-vis spectra were recorded on an Ocean Optics USB4000 spectrometer with an Ocean Optics ISS light source. Steady-state emission spectra were collected at room temperature using a PTI QuantaMaster 4 fluorescence spectrophotometer equipped with a Model 810 PMT detector. The spectra of $[\mathbf{1}]^+$ were measured in CH_2Cl_2. Quantum yields were measured using fluorescein as a standard in 0.1 M NaOH solution. Quantum yields obtained for [**1**][OTf] is 26% in CH_2Cl_2.

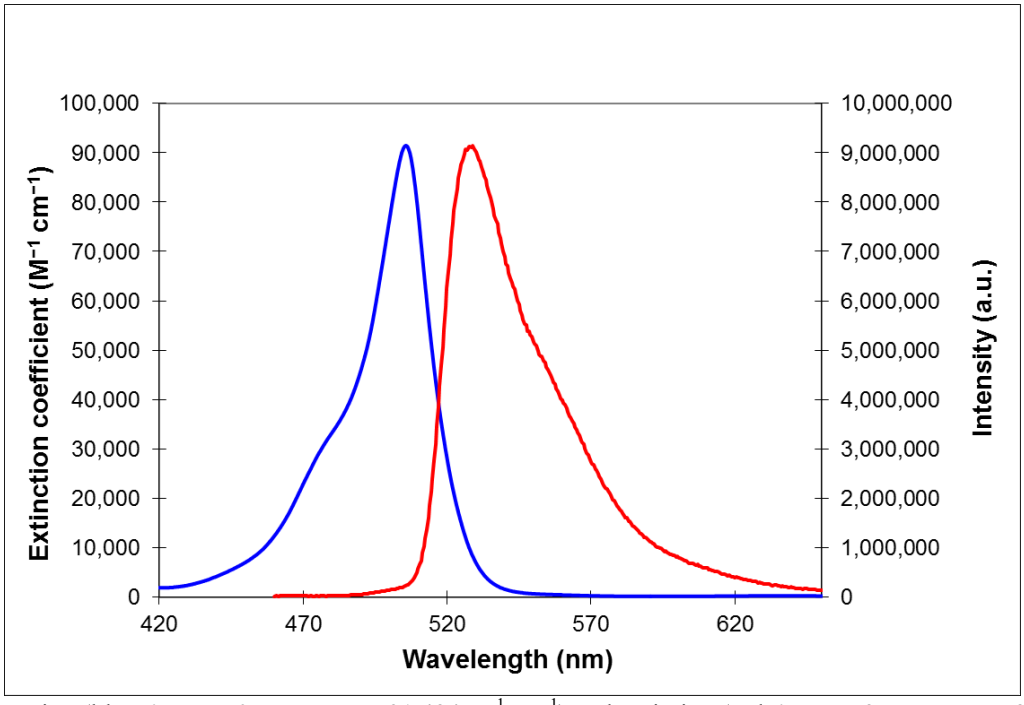

Figure S2. Absorption (blue, λ_{max} = 505 nm, ε_{max} = 91,424 M^{-1} cm^{-1}) and emission (red, λ_{max} = 527 nm, Φ_{em} = 26%) spectra of [**1**][OTf] in CH_2Cl_2.

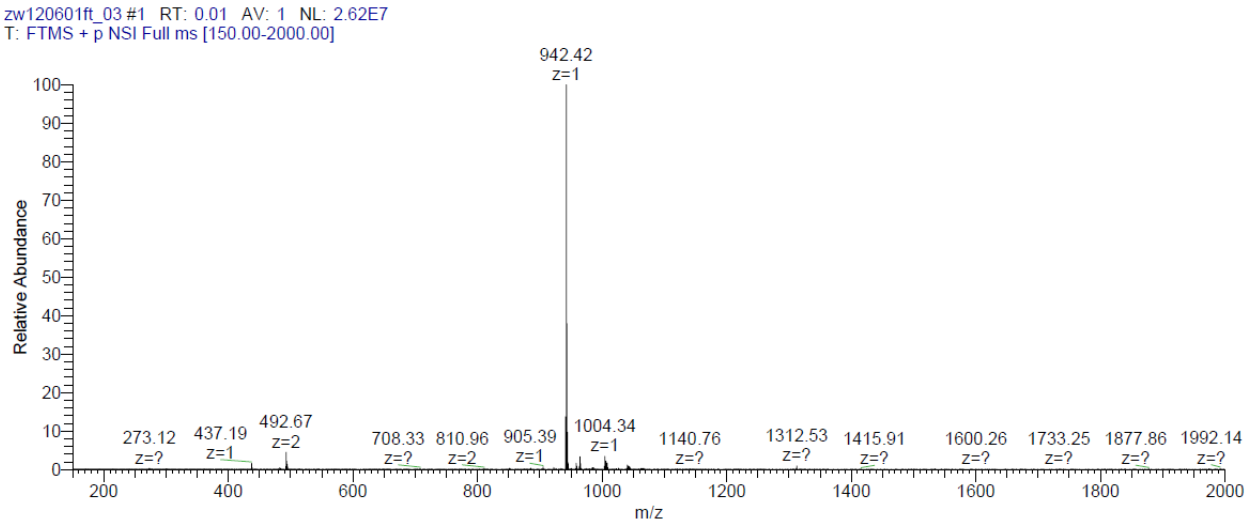

Figure S3: The mass spectra of **2**-RGD standard.

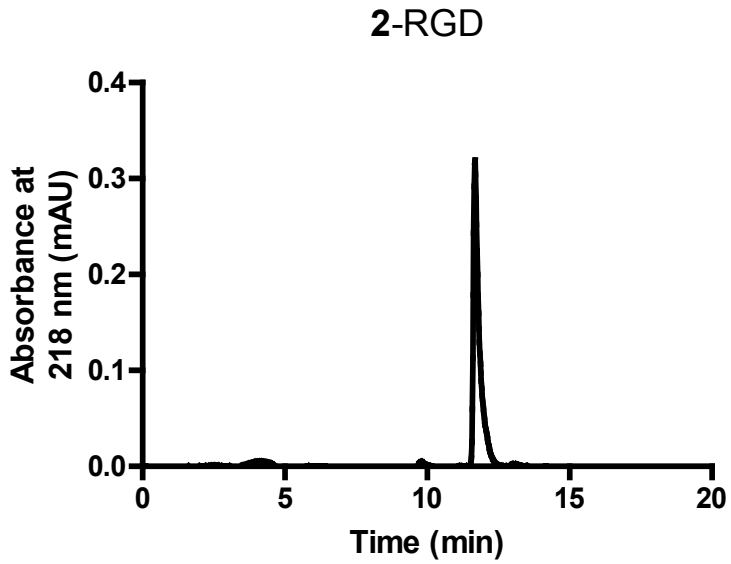

Figure S4. Analytical UV-HPLC profile of **2**-RGD.

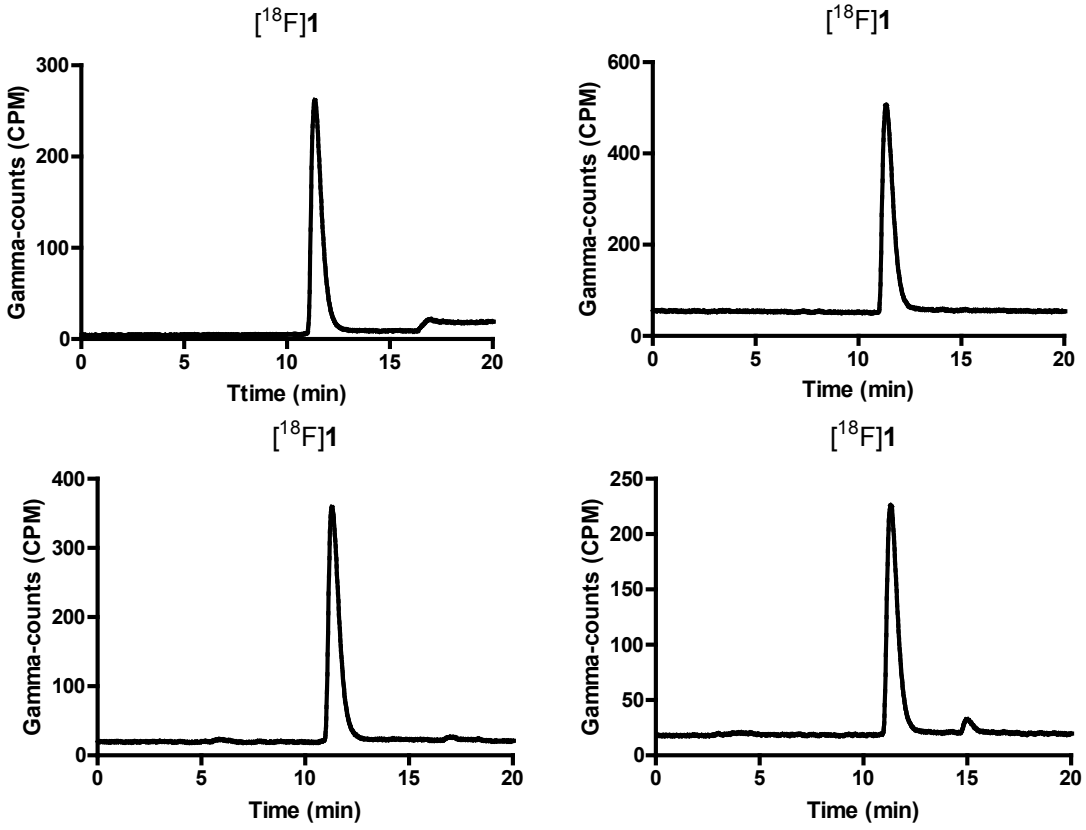

Figure S5. Four consecutive analytical HPLC profiles of crude labeling reaction for [^{18}F]**1**$^{+}$ using the reaction condition in entry 8 table 1. The following HPLC gradient is used for analysis: the flow was 1 mL/min, with the mobile phase starting from 70% solvent A (0.1% TFA in water) and 30% solvent B (0.1% TFA in MeCN) (0–2 min) to 5% solvent A and 95% solvent B at 22 min.

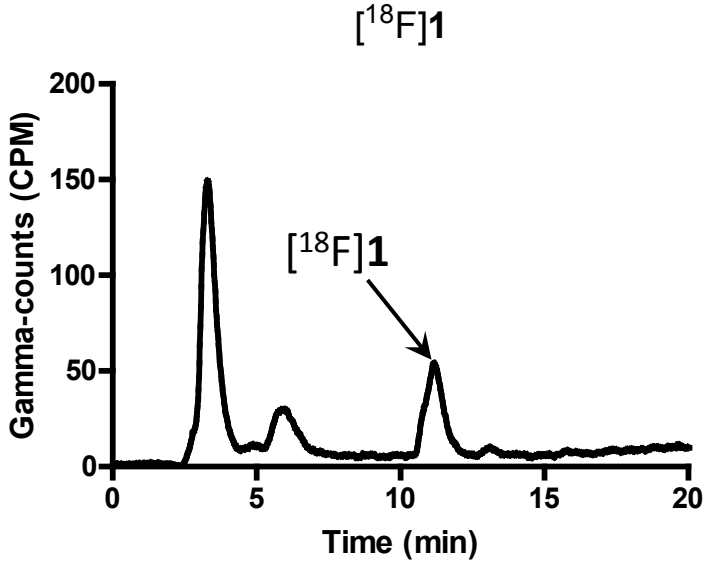

Figure S6. Radio HPLC profile of crude labeling reaction for [^{18}F]**1** using the reaction condition in Entry 5 table 1. The HPLC mobile phase gradient is the same as Figure S5.

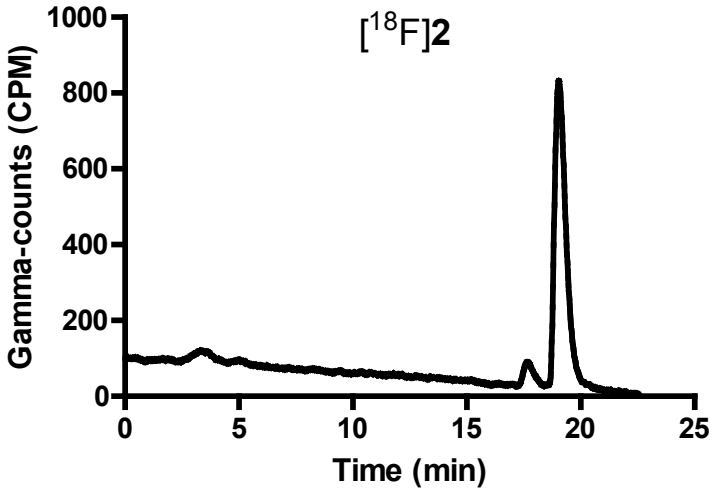

Figure S7. The quality control (QC) of [^{18}F]**2** (Radio-HPLC trace).

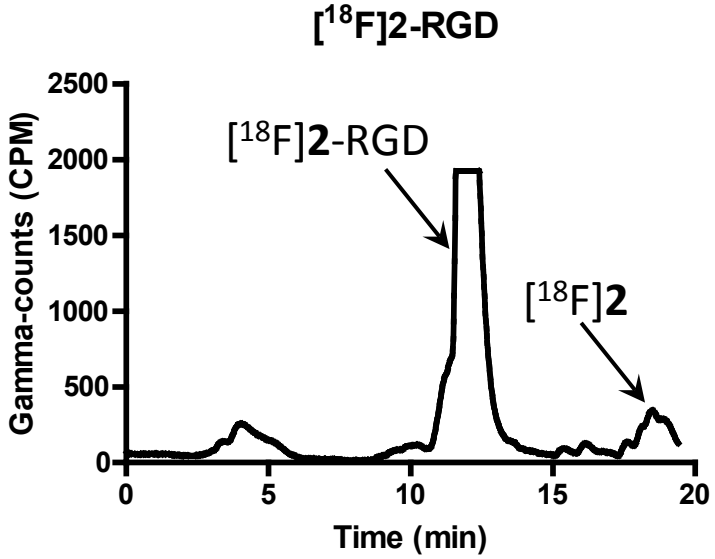

Figure S8. HPLC purification of [^{18}F]**2**-RGD (Radio-HPLC trace).

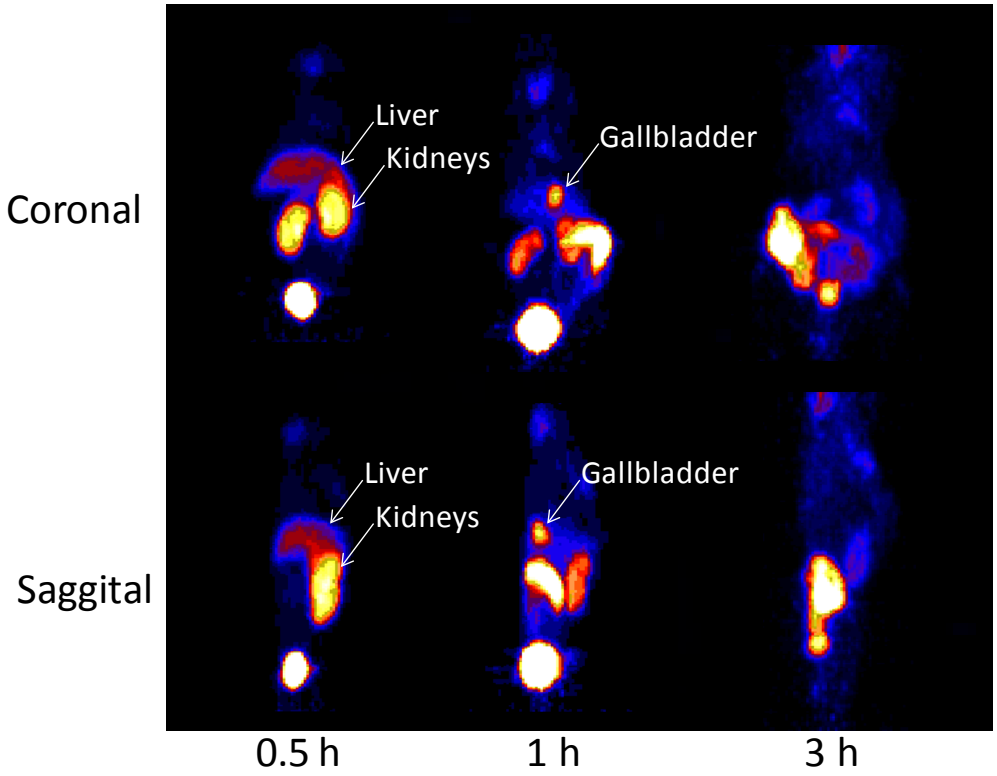

Figure S9. PET images of a mouse injected with [^{18}F]**1**$^{+}$. No detectable bone uptake is observed up to 3 h post injection. All images shown are 2D projection instead of a single slice of the scan.

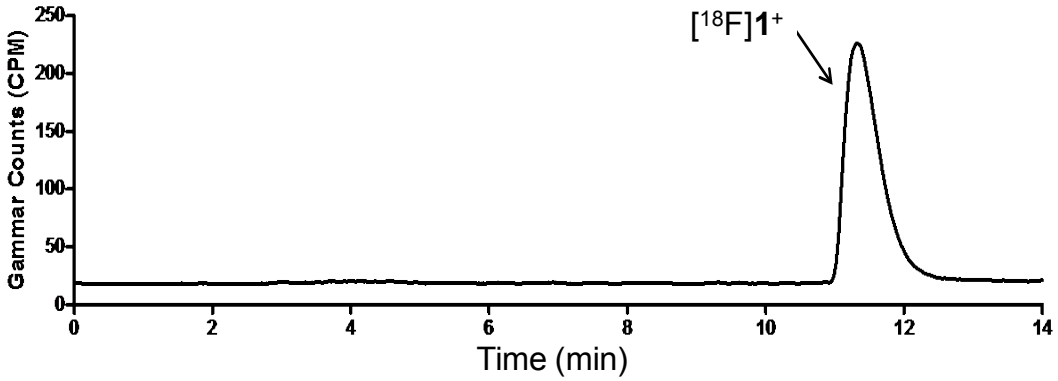

Figure S10. Radio HPLC trace of [^{18}F]**1**$^{+}$ after 6 h incubation in 1×PBS stability at 37 °C.

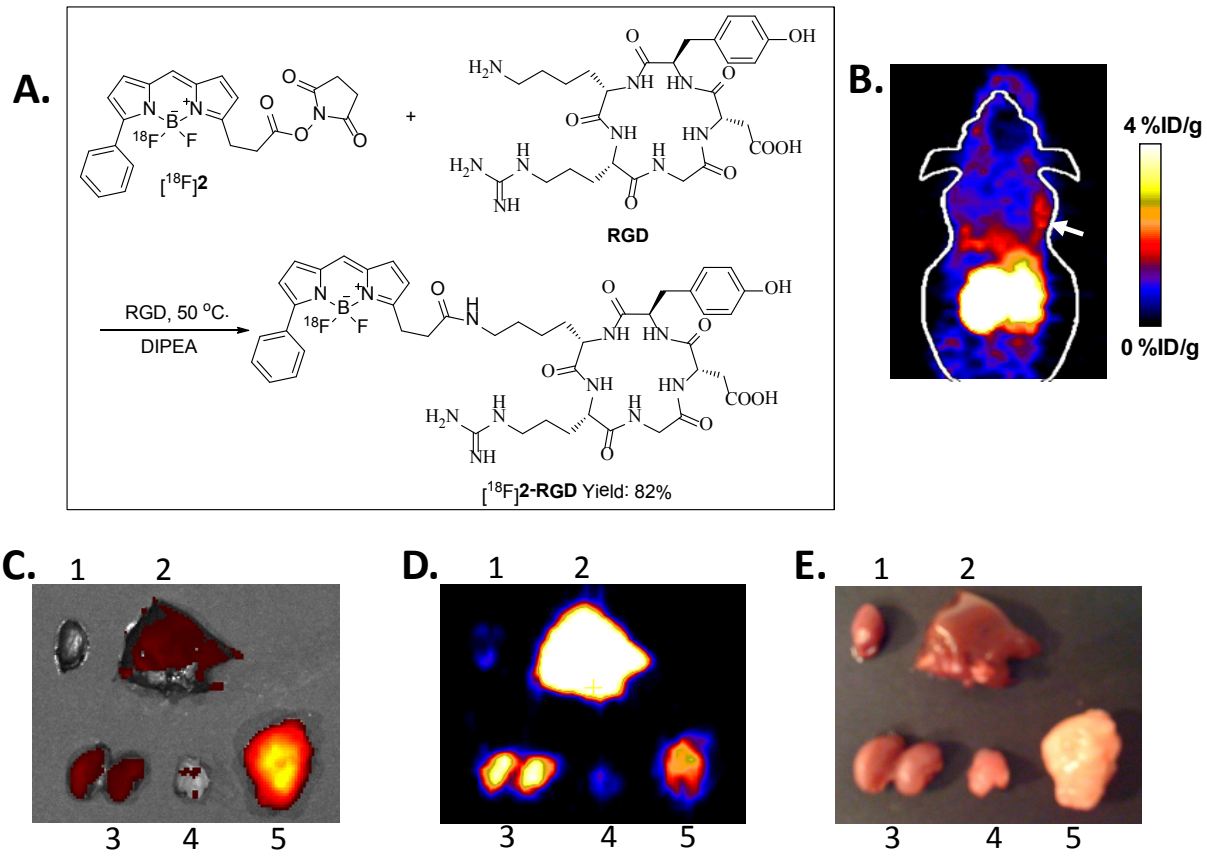

Figure S11. (A)^{18}F-labeling RGD peptide via [^{18}F]**2**. (B) Decay-corrected coronal microPET image 30 min after injection of 50 μCi of [^{18}F]**2**-RGD into a U87MG tumor-bearing nude mice. (C) *Ex vivo* fluorescence imaging of major organs and tumor 0.5 h after injection of [^{18}F]**2**-RGD into a U87MG tumor bearing nude mice. (D) *Ex vivo* microPET imaging of major organs and tumor 0.5 h after injection of [^{18}F]**2**-RGD into a U87MG tumor-bearing nude mice. (E) Bright field of the major organs and tumor. *For PET imaging, tissue penetration of the signal is not a limitation. For optical imaging, the tumor has much lighter color compared with the liver and kidneys (E), which would make the absorption of optical signals less significant in the tumor. This difference would lead to increased tumor to liver/kidney ratio as a large amount of light would be absorbed in these organs, which would lead to inaccurate correlation with PET imaging.*